Optimizing the Width and Compressive Strength of Artificial Protective Pillar in the Mining of Medium-Thick Coal Seams in Quang Ninh Using the Numerical Model

BUI Manh Tung[1)], DINH Van Cuong[2)]*

[1)] Faculty of Mining, Ha noi Univesity of Mining and Geology, Hanoi, Vietnam
[2)] VietNam National Coal – Mineral Industries Holding Corporation Limited, Hanoi, Vietnam
* Corresponding author: buimanhtung@humg.edu.vn

http://doi.org/10.29227/IM-2023-02-23

Submission date: 23-08-2023 | Review date: 19-09-2023

Abstract

Currently, in many countries with the coal mining industry, the technology of using artificial pillars has been successfully applied to replace coal pillars to protect the entry gate road, thereby reducing the rate of resource loss, as well as the cost of entry gate road, and mining costs. However, in order to optimize the required width and compressive strength of artificial pillars with thickness, slope angle and mining depth, more detailed studies are required for each specific geological condition. This research uses Phase 2 numerical simulation software to analyze the stability of artificial protective pillar of the roadway prepared in the mining of medium-thick coal seams in the Quang Ninh coal region (Vietnam). The research results show that the relationship between the width of the artificial pillar and the slope angle follows the rule of a linear function. The size of the artificial protection pillar increases according to the mining depth. When the mining depth is 350m, the size of the pillar changes from 1.0 ÷ 2.4m, and to 1.4 ÷ 2, 8m at a depth of 500m. When the slope angle increases, the required pillar width also increases. That is due to the fact that at a large slope angle, the pressure acting on the pillar is not at the center, but deflects to the side adjacent to the entry gate road that needs to be protected, the compression force is not distributed evenly. The required compressive strength of the artificial pillar varies according to the condition of the slope angle, when the seam slopes 10°, the required compressive strength is from 8 to 12 MPa, when the slope angle increases to 20°, the required compressive strength of the pier increases to 18 ÷ 28 Mpa, but when the slope angle increases to 35°, the required compressive strength of the pillar tends to decrease to 16 ÷ 17 MPa. Thus, when operating in the corresponding conditions, it is necessary to choose the size and required compressive strength of the artificial pillar to ensure the working capacity of the pillar.

Keywords: *medium thick coal seam, entry gate road, artificial support pillar, pillar width, compressive strength*

1. Introduction

The loss rate in underground mining technology in Quang Ninh coal area is currently at over 20%, mainly concentrated in coal pillars protecting the transport roadway (Cuong et al.,2019). This rate is relatively high, significantly affecting the efficiency of mine construction investment and wasting non-renewable resources.

In many countries, a technological solution has been successfully applied to use artificial pillars to replace coal pillars to protect the roadway. In that technology, in order to simultaneously exploit coal in the protection pillar and maintain the transport roadway as a ventilation roadway for the next coalface, the coal pillar will be replaced by an artificial pillar formed from a strip of rock inserts, clusters of columns, cribs, chemical materials or concrete mortar mixes. In addition to reducing the rate of resource loss, the solution of using artificial pillars also allows reducing the cost of preparing roadway meters, reducing 01 main entry, equivalent to about 50% of the cost and the cost of mining.

Hu (2012) utilized statistical analysis methods to analyze more than 20 mines that utilized waste rock backfilling in China, examining the technical characteristics of different backfill materials for protecting underground mine structures. The study identified that production capacity, size of backfill material, extraction ratio, extraction cost, backfill efficiency, degree of mobility, deformation, and protected area are fundamental indicators for evaluating the effectiveness of backfill in mines. Based on the practical experience, Song. (2010) concludes that the reasonable load-bearing capacity of the material used for artificial pillars is the determining factor for their effectiveness. Waste rock in underground mines is one of the main backfill materials that contribute to the formation of pillars with high strength. Some studies on coal pillar recovery have also recently been carried out. Zhou et al.(2019) proposed the use of a sand-based backfilling body to recover the remaining coal pillars and analyzed the principle involved in the use of sand-based backfilling bodies to maintain the stability of the stope. Ma et al.(2017) proposed the use of solid backfill to replace the coal pillars in the lower part of an industrial square to provide effective surface-subsidence control while Sun et al.(2018) proposed the cemented paste backfilling method to recover short-strip coal pillars and studied the stability conditions of the impermeable layer.

In the study on the degradation law of cemented artificial pillars as a replacement for protective inter-block coal pillars, Chi et al.(2023) employed the Flac3D model to simulate real conditions in a mine in Shanxi, China. The results demonstrated that with a pillar width of 14m, the cemented artificial pillars could sufficiently bear the load requirements, and the surrounding rock mass remained relatively stable. The field monitoring at the experimental site confirmed the feasibility

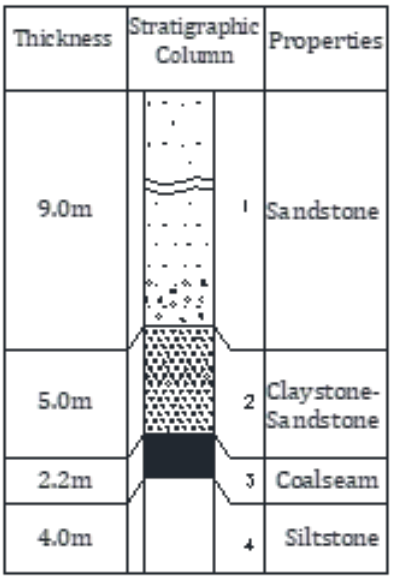

Fig. 1.1. The typical geological column

Fig. 1.1. The typical geological column

Materials	Density, T/m³	Elastic module, MPa	Poisson index	Tensile strength, MPa	Internal friction angle, degree	Adhesive force, MPa
Coal	1,64	2000	0,25	0,1	28	1,0
Claystone	2,65	3000	0,29	0,2	29	1,4
Siltstone	2,66	4270	0,23	0,42	31,47	2,6
Sandstone	2,71	4000	0,21	0,1	33,28	5,0
Conglomerate, gritstone	2,66	4000	0,20	0,1	33,5	4,8
Post-caving coal and rock	1,70	30	0,07	0	30	0

of using cemented artificial pillars as a replacement for protective inter-block coal pillars.

However, there have been few published results describing the recovery of replacing protective inter-block coal pillars generated by the short wall block mining process, hence further analysis and exploration are needed.

The research works to reduce coal loss in the pipeline protective pillar carried out in Vietnam have mainly been in the direction of reducing the size of the pillar, driving new ventilation roadway following the areas that have been exploited, or making the most of the protection pillars while exploiting the blast roadway. Recently, the diagram of mining technology without leaving protection pillars has also been studied and proposed but has not been implemented in practice. Therefore, it is necessary to have detailed studies on determining the parameters of the artificial pillars to protect the preparatory roadway during the mining process at the underground mines in Quang Ninh region in order to maximize the resources and improve production efficiency.

The artificial pillar, replacing the coal pillar, must ensure resistance against the mining pressure exerted on it, taking into account the geological conditions of the construction area of the roadway and the depth at which the roadway is located. If the artificial pillar is constructed using materials with low compressive strength, the width of the pillar will need to be large, resulting in a greater amount of material to be transported, increased labor intensity, and higher construction costs. Therefore, two fundamental parameters of the artificial pillar need to be determined: (1) the width dimension of the pillar (B) and (2) the required compressive strength of the pillar (P).

In terms of the research subject, the utilization of materials with high compressive strength for the artificial pillar represents a significant advancement and a high level of reliability within the mining industry. The application of this form of artificial pillar has become a prevailing trend, and it is prioritized whenever conditions allow. Therefore, in this context, the article delves into a comprehensive investigation and analysis to determine the optimal parameters for the implementation of artificial pillars utilizing materials with high compressive strength.

2. Characteristics of rock geological conditions

The geological conditions consist of coal seams and common rock types within the stratigraphy of the Quang Ninh region (such as clay, shale, sandstone, conglomerate, siltstone, etc). The average thickness of the coal seam is 2.2 meters, while the average thickness of the immediate roof rock is 5.0 meters, and the main roof rock is 9.0 meters. The coalface employs a longwall mining system, with pressure control achieved through the method of fully caving. The typical geological column is depicted in Figure 1.1.

The main geomechanical properties of the real rock mass in the Quang Ninh coalfield is reflected in Table 1.

3. Reseach on the optimal compressive strength of artificial pillars to protect roadway

Currently, in the field of stability analysis of the rock mass surrounding underground mining voids and the design of support structures for mining areas in coal mines, several calculation software programs based on fundamental math-

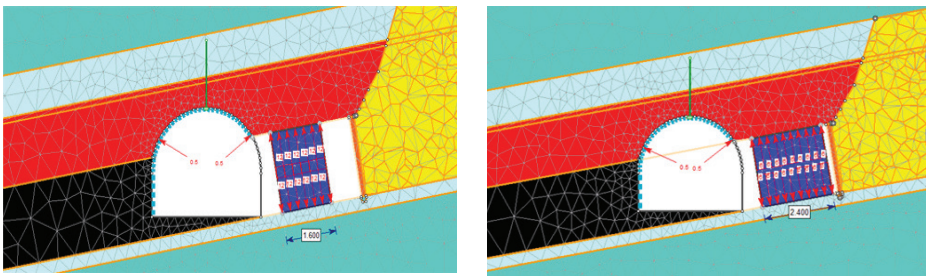

The pillar width: B=1,6m The pillar width: B=2,4m

Fig. 2.1. The analysis model of average seam, sloping angle α = 10°

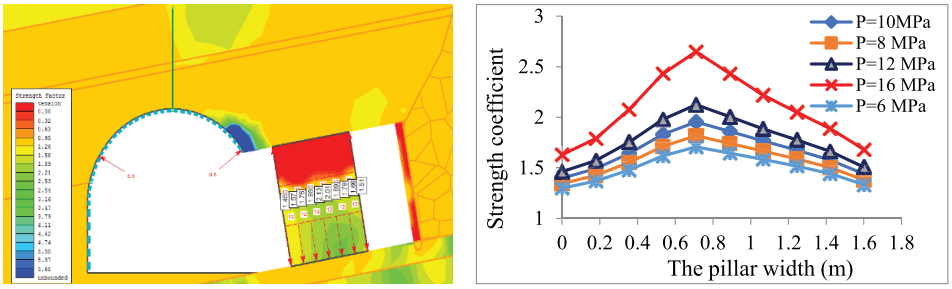

a) Strength coefficient inside the pillar b) Strength coefficient of the protective pillar

Fig. 2.2. Strength coefficient of the protective pillar (B = 1,6m, α= 10°)

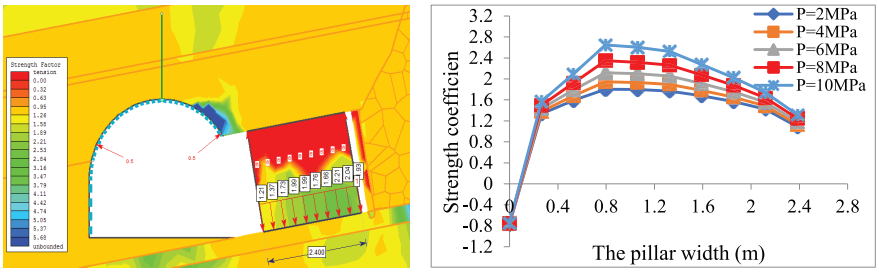

a) Strength coefficient inside the pillar b) Strength coefficient of the protective pillar

Fig. 2.3. Compressive strength and strength coefficient of the protective pillar (B = 2,4m, α= 10°)

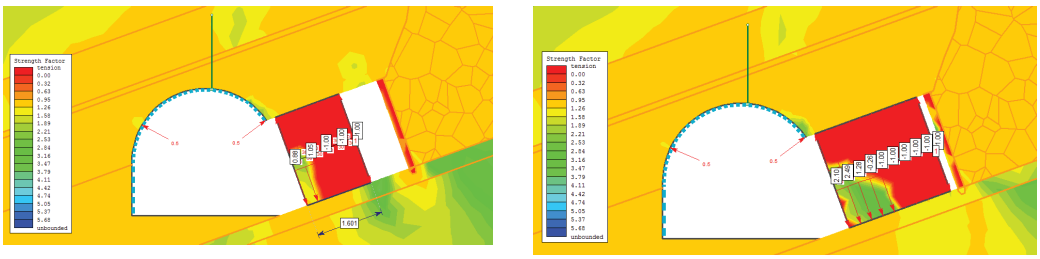

a) Safety coefficient of the pillar when B = 1,6m, P = 30MPa b) Safety coefficient of the pillar when B = 2,4m, P = 20MPa

Fig. 2.4. The strength coefficient of protective pillar, α = 20°

ematical methods such as the finite element method, finite difference method, limit equilibrium method, boundary element method, discrete element method, etc., have been widely used. Some notable software programs include Phase 2, Ansys, Abaqus, UDEC, Flac, etc. In this article, the Phase 2 software (based on the finite element method) is chosen to analyze the necessary stability of the artificial support column, taking into account geological and engineering parameters such as thickness, dip angle of seam, mining depth, and required compressive strength of the artificial pillars.

3.1 Numerical model development

The working capacity of the artificial pillars is influenced by various geological and mining engineering factors such as the thickness and dip angle of the seam, the mechanical properties of the surrounding rock, the mining depth, hydrogeological conditions, gas content in the mine, coal self-ignition capacity, and the applied mining technology. Within the scope of this research, the focus will be on selecting and limiting the typical input parameters based on the current mining conditions in the Quang Ninh coal region. These parameters greatly affect the working capacity of the artificial pillar, namely the

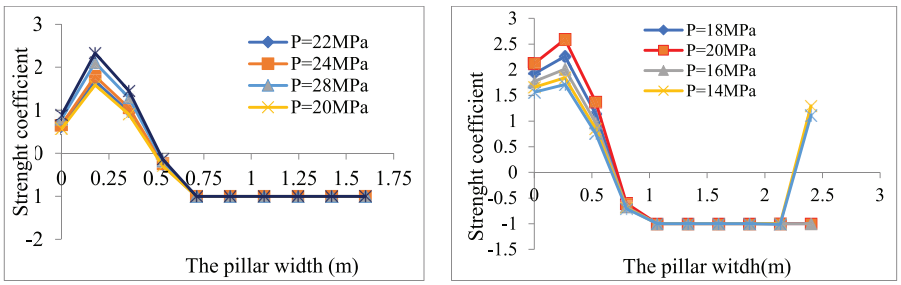

a) B = 1,6m b) B = 2,4m

Fig. 2.5. The relationship between the strength coefficient and the compressive strength, α = 20°

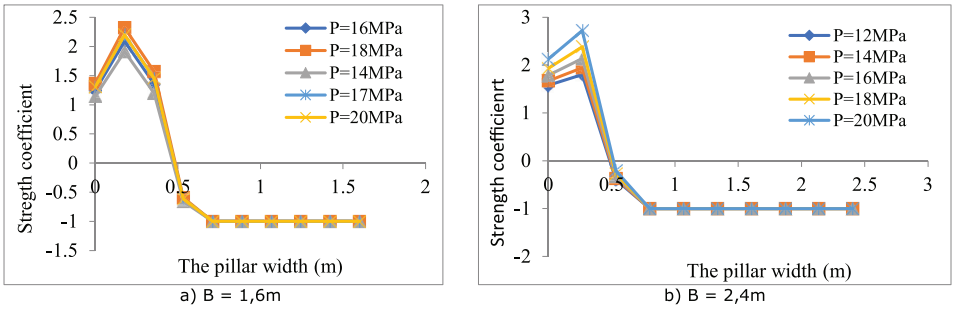

a) B = 1,6m b) B = 2,4m

Fig. 2.6. The relationship between the strength coefficient and the compressive strength, α = 35°

Tab. 2.1. Research results on the optimal compressive strength of the artificial pillar under conditions of medium-thick coal seam

Pillar width	Seam slope angle		
	10°	20°	35°
1,6m	12 MPa	28 MPa	17 MPa
2,4m	8 MPa	18 MPa	16 MPa

seam thickness, dip angle, and mining depth. Specifically:

For the seam thickness factor, a case study with an average thickness of 2.2m will be chosen.

For the dip angle factor, the range of dip angles will be limited to 35 degrees, with intervals of 10 degrees, 20 degrees, and 35 degrees.

Regarding the mining depth, two values will be selected: 350m (representing the common mining level in current mines) and 500m (representing the depth of sustained mining levels).

The seam consists of claystone, siltstone, sandstone, and the seam of the pillar are composed of siltstone and sandstone (Figure 1.1, Table 1.1). The numerical analysis model for the problem has a width of 33.509m and a height of 24.025m, ensuring that the distance from the mine boundary is equal to (5–6) times half the width of the roadway so that the influence of the roadway on the surrounding rock mass is negligible. As the protected roadway is located at a significant depth, the overlying soil and rock in the model are replaced by an equivalent load with a value of:

$$p = (H - h).\gamma; \text{ MPa} \quad (2.10)$$

Where:

H – the depth of roadway placement, H1 = 350m; H2=500m

h – height from the top of the roadway to the top of the model, h = 13,375m

γ – weight of the volume of rock layers above the roadway, average γ = 0,026MN/m³;

Applying the formulae 2.10, the vertical load is determined to change according to the length: p_1=8,75MPa; p_2 = 12,06MPa.

The directional control of the artificial pillar width is constrained within the range of (0.7-1.1) times the height of the face (Niełacny, 2009 and Rak, 2017). With a corresponding mirror aperture height of 2.2m, the artificial pillar width is determined to be 1.6m and 2.4m, allowing for the determination of the appropriate compressive strength of the artificial pillar under slope conditions of 10°, 20° and 35°.

To describe the width of the protective pillar, the model utilizes a separate rock layer with the characteristics of artificial rock to establish and hypothesize the variation in soil pressure caused by the artificial pillar. The roadway gallery is supported by SVP-22 steel, and the reinforced two-column steel support system of the roadway is described in the model using concentrated forces generated by the support columns, with corresponding values of 0.5 MN/m2 or 50 tons/m². The anchorage structure and the SVP steel are simultaneously described in the model of the problem. The numerical model diagram is created using Phase 2 software for the cases described in Figures 2.1.

3.2 Result analysis

As mentioned above, the working capacity of the artificial pillar is represented by the stability coefficient, which refers to its ability to maintain stability under the load of the mine. The stability coefficient of the pillar is determined by dividing the ultimate load-bearing capacity of the pillar by the load applied to the pillar from the mine. For the design of stable protective pillars in underground coal mining, a stability coefficient value of ≥ (1.5 to 2.0) for the rock pillar is considered acceptable (Reed et al., 2017; Simon et al.,2019 and Bieniewski., 1992). Depending on the complexity, characteristics, and

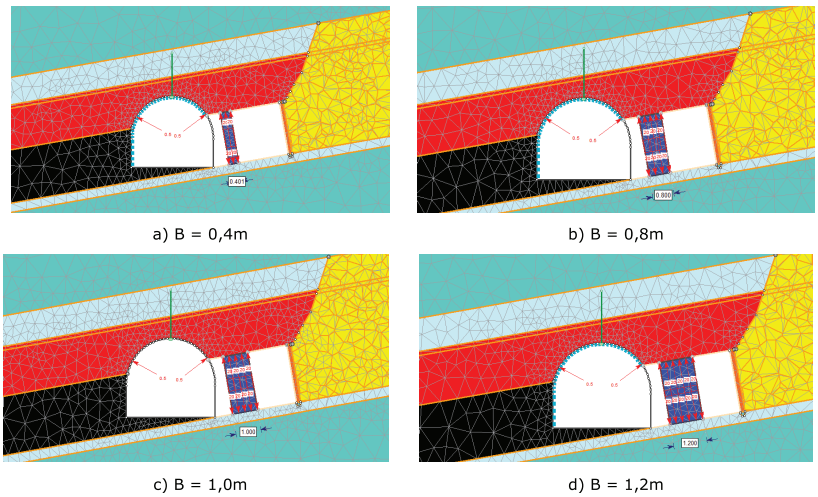

Fig. 2.7. Model to determine optimal pillar width

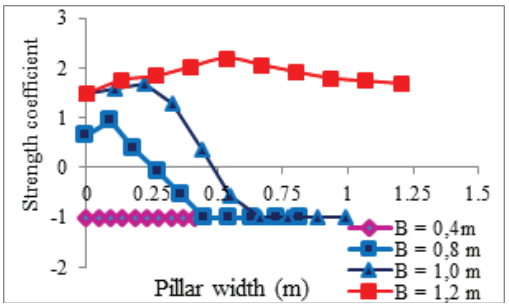

Fig. 2.8. The relationship between the strength coefficient and the protective pillar, α = 10°, H = 350m, P = 20MPa

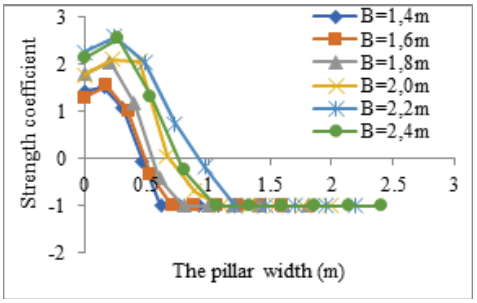

Fig. 2.9. The relationship between the safety factor and the width of the protective pillar, α =20°, H = 350m, P = 20MPa

importance of the protected gallery, a value greater than 2 can be selected. Due to the complex geological conditions in the underground coal mines of the Quang Ninh region, the author chooses a stability coefficient of 2 to determine the optimal compressive strength of the artificial pillar in the numerical model. Thus, in the models, the assumed compressive strength value of the pillar will be varied until the stability coefficient of the pillar reaches a value ≥ 2, indicating that the pillar meets the required stability criteria. The detail results are as followed:

In the case of a slope angle of 100, with an artificial protective pillar width of B=1.6m, through numerical analysis, the research results indicate the strength coefficient values of the materials in the pillar as shown in Figures 2.2.

Observing the results on the graph, it can be seen that when the compressive strength of the protective pillar is ≥ 12MPa, the stability coefficient at the midpoint of the pillar has a value > 2.0. This represents the minimum or optimal compressive strength value that the pillar must achieve.

In the case of a slope angle of 10o and an artificial protective pillar width of 2.4m, a similar analysis has been conducted with the analytical model and stability coefficient as shown in Figures 2.3.

It can be observed in the Figure 2.3 that when the compressive strength of the protective pillar is ≥ 8MPa, the stability coefficient of the pillar has a value ≥ 2.0. This represents the minimum compressive strength value that the pillar must achieve in the case of a width of 2.4m. From the graph in Figure 2.3, it is also evident that as the width of the protective pillar increases, the load-carrying capacity of the pillar increases, thereby reducing the required compressive strength. This is consistent with practical observations, as smaller protective pillars require higher strength, while larger ones can have reduced compressive strength requirements.

In the case of a slope angle of 20°, with protective pillar widths of B = 1.6m and B = 2.4m, through numerical modeling, the research content establishes a model for determining the optimal compressive strength of the pillar as shown in Figures 2.4.

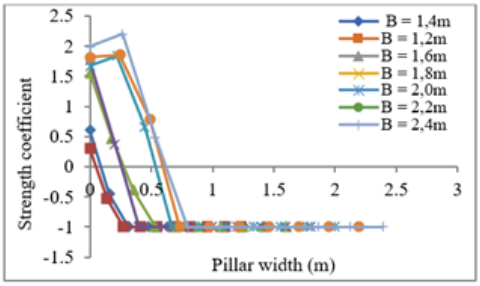

Fig. 2.10. The relationship between the strength coefficient and the protective pillar width, α = 35°, H = 350m, P = 20 MPa

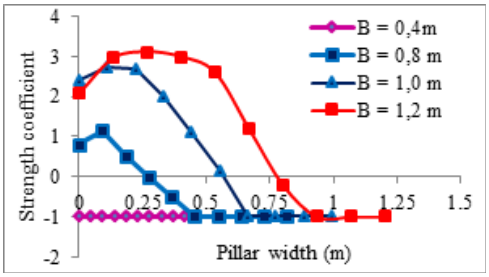

Fig. 2.11. The relationship between the strength coefficient and the protective pillar width, α = 10°, H = 350m, P = 30MPa

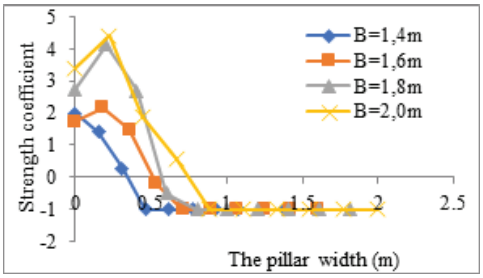

Fig. 2.12. The relationship between the strength coefficient and the protective pillar width, α =20°, H = 350m, P = 30MPa

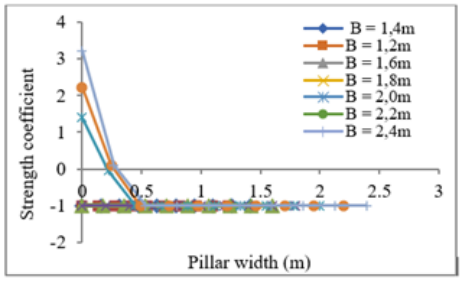

Fig. 2.13. The relationship between the strength coefficient and the protective pillar width, α =35°, H = 350m, P = 30 MPa

Observing the distribution of the strength coefficient in the protective pillar, it is found that when the slope angle of the seam increases to 20°, the distribution of the safety factor skews towards the left side of the pillar, with the region of distribution located approximately one-third of the width of the protective pillar. By conducting multiple models with different values of the compressive strength of the protective pillar, the research yields the relationship between the strength coefficient of the protective pillar and the width of the protective pillar for two cases: B = 1.6m and B = 2.4m, as shown in Figures 2.5.

Observing the results from the two graphs in Figures 2.5, it is observed that in the case of B = 1.6m, for compressive strength of the protective pillar P ≥ 28MPa, the strength coefficient ensures stability. In the case of B = 2.4m, the necessary compressive strength of the protective pillar is P ≥ 18MPa.

Next, further research is conducted for a seam slope angle of 35 degrees and pillar widths B = 1.6m and B = 2.4m. By performing multiple model simulations, the relationship between the strength coefficient of the protective pillar and the varying values of the compressive strength of the protective pillar is obtained, as described in Figures 2.6.

Observing the results from the graphs in Figures 2.6, it is noted that similar to the case of a 20 degree slope angle, when the slope angle of the seam increases to 35 degrees, the distribution of the strength coefficient in the protective pillar skews further towards the left side of the pillar. The region of distribution is concentrated approximately between one-third to one-fifth of the width of the protective pillar. The optimal compressive strength required to ensure a strength coefficient ≥ 2.0 is P ≥ 17MPa for B = 1.6m, and P ≥ 16MPa for B = 2.4m in the case of an medium-thick coal seam and a slope angle

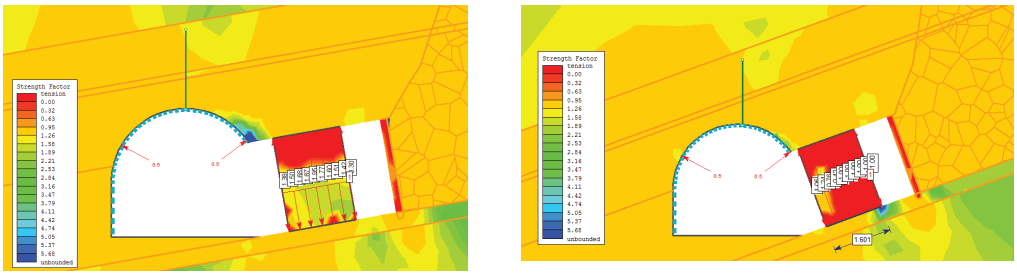

a) Slope angle α = 10° b) Slope angle α = 20°

Fig. 2.14. The distribution of strength coefficient, mining depth of 500m

of α = 35 degrees. These values are considered optimal for the protective pillar under these conditions.

The research results determining the optimal compressive strength of the artificial pillar are presented in Table 2.1.

The research results presented in Table 2.1 show that the required compressive strength of the artificial pillar under conditions of a 10° slope angle (8-12 MPa) is lower than in other cases. The reason is that the strength coefficient is evenly distributed across the entire width of the pillar, allowing for its load-bearing capacity to be fully utilized. When the slope angle increases to 20°, the strength coefficient skews towards the left side (adjacent to the protective boundary), resulting in uneven pressure distribution across the width of the pillar. To prevent failure, the required compressive strength of the pillar needs to be increased (18 ÷ 28 MPa). However, when the slope angle reaches 35°, there is a trend of decreasing the required compressive strength of the pillar. The reason is that at higher slope angles, there is a significant eccentric pressure, leading to a reduction in the vertical pressure acting on the pillar while increasing the pressure on its sides.

4. Determining the optimal size of the artificial protective pillar for roadway protection

Based on the results presented in Table 2.1, in comparison with the conditions of the coal seams in the majority of the Quang Ninh region, which are predominantly inclined with slopes ranging from 15o to 35o, and considering the overall experience of using artificial pillars worldwide, the construction materials for the pillars commonly have compressive strengths ranging from 20 to 40 MPa. Therefore, for the purpose of studying and determining the optimal width of the artificial pillars, the research has selected compressive strengths of 20 MPa and 30 MPa for the construction materials of the pillars.

As analyzed in the previous section, this section will focus on selecting the optimal width of the protective pillars under the assumption of predetermined compressive strengths of 20 MPa and 30 MPa.

4.1. Analysis model for the case of the medium-thick coal seam, artificial pillar compressive strength of 20 MPa, and mining depth of 350m and slope angle of 10° , 20°, 35°

Based on the above assumption, the research focuses on a fixed artificial pillar compressive strength of 20 MPa and varies the width of the protective pillar, B, from 0.4m until the pillar's safety factor reaches a value of ≥ 2.0. At that point, we will have the optimal width of the protective pillar, as illustrated in Figure 2.7.

In the case of artificial pillar compressive strength of 20 MPa and slope angle of 100. By analyzing the data, a chart depicting the relationship between the pillar's strength factor and the variation in pillar width is established, as shown in Figure 2.8.

Observing the results on the graph, it can be seen that when the safety factor of the pillar reaches a value of ≥ 2.0, the width of the protective pillar can be considered optimal. Correspondingly, in this case, when the width of the protective pillar, B, is 1.2m, the safety factor is 2.9. In other words, with the assumed compressive strength of the pillar of 20 MPa, the minimum (optimal) width of the protective pillar is 1.2m in the condition of medium-thick coal seam and a slope angle of 100.

In the case of the compressive strength of the pillar of 20 Mpa and slope angle of 200, the research aims to construct and develop various models while keeping P = 20 MPa constant for all models and varying the width of the protective pillar, B, as follows: 1.4m, 1.6m, 1.8m, 2.0m, 2.2m, and 2.4m. The study focuses on observing the changes in the safety factor of the protective pillar. The obtained results show the relationship between the safety factor of the protective pillar and its width, as depicted in Figure 2.9.

Observing the graph, it can be seen that the safety factor of the protective pillar is concentrated mainly in the left-third region of the pillar's width. In the case where the width of the pillar, B, is equal to or greater than (1.8 to 2.0) meters, with a pressure exerted by the protective pillar of P = 20 MPa, a safety factor of ≥ 2.0 is considered acceptable. This width is considered optimal for the protective pillar in the case of a medium-thick coal seam and a slope angle of 20°.

In the case of the compressive strength of the pillar of 20 Mpa and slope angle of 35o, by conducting a similar analysis with varying pillar widths ranging from 1.4m to 2.4m, the analytical model shows that under the conditions of a 35° slope, a pillar compressive strength of 20 MPa, the optimal width for the protective pillar is B = 2.4m (Figure 2.10).

4.2. Analysis model for the case of medium-thick coal seam, artificial pillar compressive strength of 30 MPa, mining depth of 350m and slope angle of 10°, 20°, 35°

In the case of pillar compressive strength of 30 MPa, slope angle of 10o, by varying the width of the pillar in the models from 0.4m ÷ 1.2m, the research results establish the relationship between the stability factor of the pillar and the width of the protective pillar, as shown in Figure 2.11.

Observing the results in Figure 2.11, it can be seen that when the compressive strength of the protective pillar is 30MPa, the optimal width of the pillar can be chosen as B = 1.0m. This is also consistent with reality, as the greater the load-bearing capacity of the pillar, the narrower the width of the pillar can be reduced.

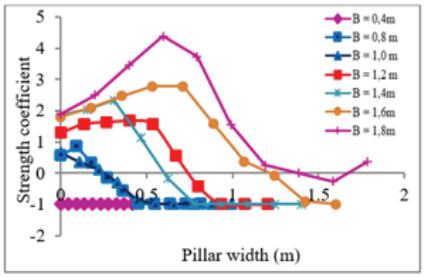

Fig. 2.15. The relationship between the strength coefficient and the width, α = 10°, H = 500m, P = 20MPa

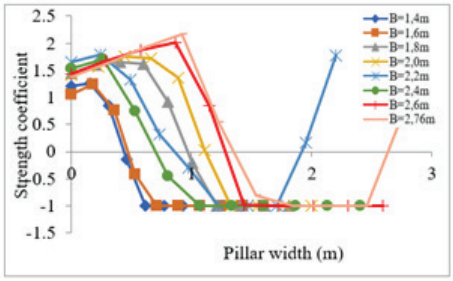

Fig. 2.16. The relationship between the strength coefficient and the width , α = 20°, H = 500m, P = 20MPa

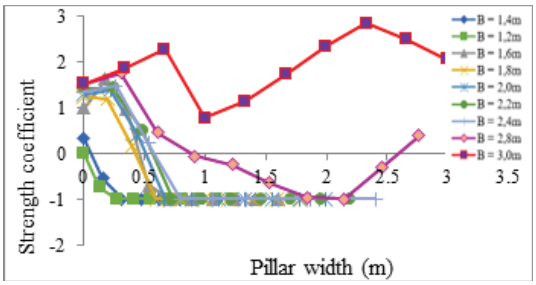

Fig. 2.17. The relationship between the strength coefficient and the width, α = 35°, H = 500m, P = 20MPa

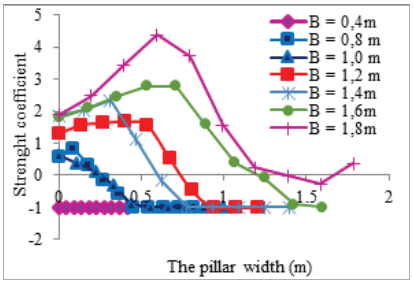

Fig. 2.18. The relationship between the strength coefficient and the width, α = 10°, H = 500m, P = 30MPa

In the case of pillar compressive strength of 30 MPa, slope angle of 20o, by keeping the pressure of the artificial protective pillar fixed at P = 30MPa and varying the width of the pillar from 1.4m to 2.0m, the research findings show the relationship between the strength coefficient of the protective pillar and the width of the pillar, as depicted in Figure 2.12. The results indicate that as the pressure of the artificial pillar increases to 30MPa, the width of the pillar can be reduced. In this case, a width of B = 1.6m ensures sufficient strength when subjected to load.

In the case of the compressive strength of the pillar of 30 MPa, slope angle of 35o. Similarly, by observing the relationship between the stability factor of the protective pillar and the width of the pillar in the case of a slope angle of α = 35° (Figure 2.13), it is found that in the case of a pillar compressive strength of P = 30MPa, the optimal width of the protective pillar is considered to be B ≥ 2.2m.

4.3 Analysis model for the case of medium-thick coal seam, artificial pillar compressive strength of 20 MPa, and mining depth of 500m

The typical numerical analysis model for the case of medium-thick coal seam is with the initial assumed pressure of P = 20MPa. After conducting the analysis, the distribution of the safety factors in the protective pillar is obtained for the respective cases. For example, the distribution of the safety factors in the protective pillar for two cases of medium-thick coal seam and a mining depth of 500m corresponding to slope angles of α = 10° and 20° can be seen in Figure 2.14.

Through analysis, the research has obtained the distribution law of the strength coefficient in the protective pillar for different cases of medium-thick coal seam, considering different slope angles α = 10°, α = 20°, and α = 35°, at a depth of 500m. These findings are depicted in diagrams from Figure 2.15 to 2.17.

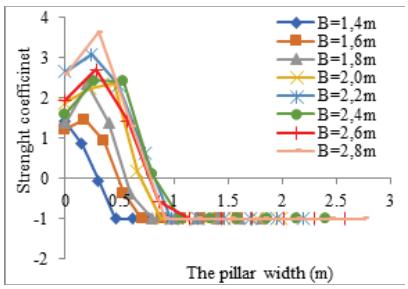

Fig. 2.19. The relationship between the strength coefficient and the width, α = 20°, H = 500m, P = 30MPa

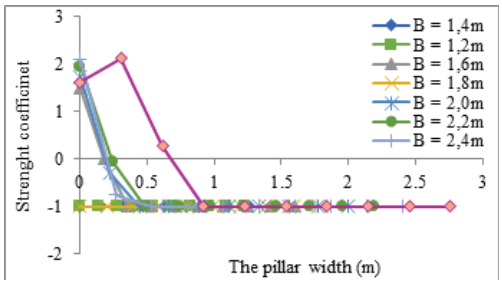

Fig. 2.20. The relationship between the strength coefficient and the width, α = 35°, H = 500m, P = 30MPa

The results obtained from figures 2.16 to 2.18 show that in the case of mining in medium-thick coal seam, with a slope angle of α = 10° (figure 2.16), the optimal width of the protective pillar is B > 1.6m. In practical terms, it is recommended to choose B = 1.8m, as it ensures a safety coefficient of ≥ 2.0 for the pillar.

For the case of a slope angle of α = 20° (figure 2.16), the optimal width of the protective pillar is considered to be B ≥ 2.76m (rounded to 2.8m). Similarly, for the case of a slope angle of α = 35° and a mining depth of H = 500m, the optimal width of the protective pillar is B ≥ 3.0m (figure 2.17).

4.4. Analysis model for the case of medium-thick coal seam, artificial pillar compressive strength of 30 MPa, and mining depth of 500m

In the case of using a compressive strength of the protective pillar of P = 30MPa, through multiple models, the research findings reveal the relationship between the safety factor and the width of the protective pillar for the condition of medium-thick coal seam with a depth of H = 500m and slope angles of 10°, 20°, and 35°, as depicted in figures 2.18 ÷ 2.20.

Observing the results in figures 2.38 to 2.40, with a compressive strength of 30 MPa and a mining depth of 500m, for a slope angle of 10°, the optimal width of the protective pillar is B = 1.4m; for a slope angle of 20°, B = 1.8m; and for a slope angle of 35°, B = 2.8m.

Summarizing the research findings, the optimal width of the protective pillar is determined based on the variation in compressive strength and the relationship between the pillar width and factors such as the slope angle and mining depth, as presented in Table 2.2.

4.5. Research result analysis for the numerical medel in case of medium-thick coal seam

The analysis of the results on the numerical model aims to determine the correlation between the research parameters obtained from Table 2.10, including the slope angle of the coal seam (α), the thickness of the coal seam (m), the mining depth (H), the compressive strength of the artificial pillar (P), and the width of the artificial pillar (B). The details are shown in Table 2.3.

To find out the relationship between the mentioned parameters, the research utilized the statistical software SPSS, IBM version 25 (Figure 2.21).

Therefore, the relationship between the artificial pillar width and the slope angle in the case of medium-thick coal seam follows a linear function as follows:

$$y = 0.0508x + 0.8829 \quad (1)$$

With a variance of $R^2 = 0.9591$.

Where:

y – Artificial pillar width, in meters (m);

x – Slope angle, in degrees.

The above function serves as a reference, allowing researchers and consultants to quickly and simply determine the dimension parameter of the artificial pillar width before carrying out the design process.

5. Assessment of the technological solution in practice

In Quang Ninh coal region, the construction of high-strength artificial pillars to replace coal pillars for roadway protection has not yet been implemented. The authors selected Khe Cham Coal Company to collaborate on deploying the technology. The chosen location for the design was section 14-5, at a depth of -170/-150, in coal seam 14-5 of Khe Cham III coal mine. The application targets the use of continuous strip-type and crib-type artificial pillars as substitutes for coal pillars in the transportation roadway. The geological and mining engineering characteristics of the design area are as follows: The designed coal seam has an average thickness of 5.6 meters, with a slope angle of 12 degrees and a strength index of f = 1÷2. The imediate rock layers consist mainly of siltstone layers with an average thickness of 9.34 meters and a strength index of f = 4 ÷ 6. The main rock layers consist of cement-

Fig. 2.15. The relationship between the strength coefficient and the width, α = 10°, H = 500m, P = 20MPa

Slope angle	Optimal width of the protective pillar, m					
	α = 10°		α = 20°		α = 35°	
H = 350m	B =1,2	B = 1,0	B = 2,0	B = 1,6	B = 2,4	B = 2,2
H = 500m	B = 1,6	B = 1,4	B = 2,8	B = 1,8	B = 3,0	B = 2,8
Compressive strength of pillar, MPa	P = 20	P = 30	P = 20	P = 30	P = 20	P = 30

Tab. 2.3. Results of key parameter values from numerical modeling

α (°)	m (*m*)	H (*m*)	P (*MPa*)	B (*m*)
10	2,2	350	20	1,2
10	2,2	350	30	1
10	2,2	500	20	1,6
10	2,2	500	30	1,4
20	2,2	350	20	2
20	2,2	350	30	1,6
20	2,2	500	20	2,8
20	2,2	500	30	1,8
35	2,2	350	20	2,4
35	2,2	350	30	2,2
35	2,2	500	20	3
35	2,2	500	30	2,8

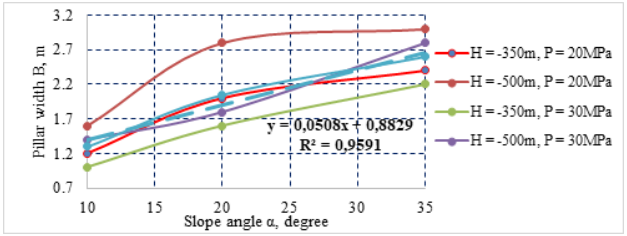

Fig. 2.21. The relationship between the parameter of artificial pillar width and the slope angle

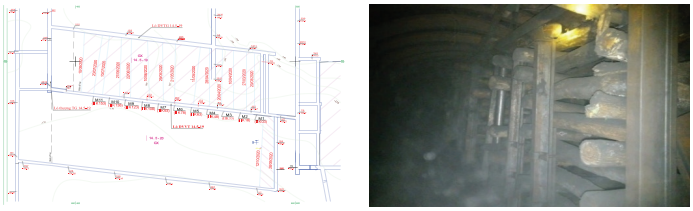

Fig. 2.22. The deployment diagram of section 14-5 using artificial support belts

ed sandstone and conglomerate with an average thickness of 40.73 meters and a strength index of f = 6 ÷ 8. The direct pillar consists of cemented silty layers with an average thickness of 3.74 meters, underlain by sandstone and conglomerate layers with an average thickness of 13.1 meters.

The implementation of the artificial pillar solution as a replacement for protective coal pillars of the transportation roadway 14-5 section was carried out from March 13, 2020 (the start of face operation) to September 10, 2020 (the end of face operation). The total length of the protected roadway was 170 meters.

Measurement results and monitoring show that within a range of approximately 40 meters in front of and behind the coalface, the deformation rate of the roadway lining is the strongest and fastest (vertical deformation rate ranges from 7 to 10 mm/day-night; horizontal deformation ranges from 8 to 20 mm/day-night). In the direction of the roadway mirror, in the area starting from the 40th meter backward, the deformation speed of the roadway lining gradually decreases (vertical deformation speed ranges from 0 to 4 mm/day-night, horizontal deformation ranges from 0 to 6 mm/day-night). From the 100th meter behind the installation roadway towards the caving area, the roadway lining is no longer moving and remains stable.

The total deformation of the roadway lining during the monitoring period reaches a maximum of 300 mm vertically and 350 mm horizontally, corresponding to a reduction in cross-sectional area of about 9.8% to 9.97%, ensuring the prescribed safety dimensions for ventilation and production purposes of the 14-6 panel.

When applying the technological solution of using artificial support columns instead of coal support columns at the 14-5 roadway, an additional 19,951 tons of coal can be extracted from the prepared support columns, increasing the total exploitation output of the designed area to 67,451 tons. Additionally, it will bring some technical benefits such as reducing the loss rate to only 14%, nearly three times lower than expected (39%); the preparation cost per meter of the roadway is also reduced to only 6.3m/1000 tons of coal, nearly 1.9 times lower than the plan (8.19m/1000 tons of coal).

6. Conclusion

The research results on the basic parameters of the artificial pillar in the case of the medium-thick coal seam in coal mining reveal the following:

1) The size of the artificial pillar varies with the increasing depth of mining. For a mining depth of 350m, the pillar size ranges from 1.0m to 2.4m, while for a mining depth of

500m, it increases from 1.4m to 2.8m. This finding agrees well with the theoretical and practical aspects of coal mining in the Quang Ninh region.

2) As the slope angle of the seam increases, the required pillar width also increases. This is because, at higher slope angles, the pressure on the pillar shifts away from the central axis towards the side adjacent to the mining face (downward along the slope direction). Consequently, the compressive force is not evenly distributed throughout the entire pillar body. To ensure the required internal stability, the pillar width needs to be increased.

3) Increasing the pressure or compressive strength of the protective pillar results in a reduction in the width of the artificial pillar. The relationship between the width of the artificial pillar and the slope angle in the case of a medium-thick coal seam follows a linear function: $y = 0.0508x + 0.8829$.

7. Acknowledgements

The paper was presented during the 7th Pol-Viet 2023 International Conference Scientific-Research Cooperation between Poland and Vietnam, 18-20.10.2023, Krakow, Poland.

Literatura – References

1. Cuong, D.V., Thanh, V.T., Tuan, A.N., 2019. Study on the possibility of using artificial pillars to replace the protection coal pillar of the preparationroadways during the mining process at underground coal mines in Quang Ninh region, Vietnam. Journal of the Polish Mineral Engineering Society, http://doi.org/10.29227/IM-2019-02-73.
2. HU, B.N., 2012. Backfill Mining Technology and Development Tendency in China Coal Mine. Coal Science and Technology. Vol. 40 No. 11. DOI: 10.13199/j.cst.2012.11.7.hubn.006.
3. Song, Z.Q, Cui, Z.D., Xia. H.C., Tang, J.Q., Wen, Z.J., 2010. The fundamental theoretical and engineering research on the green safe no coal pillar mining model mainly using coal gangue backfill. Journal of China Coal Society, No.05, Vol.35. DOI:10.13225/j.cnki.jccs.2010.05.017
4. Dinh, V.C., Nguyen, A.T., Tran, V.T., Nguyen, H.Ng., Duong, D.H., 2021. Applying Artificial Pillar to Replace the Coal Pillar Protecting Roadway to Increase Production Efficiency and Sustainable Development in the Vietnamese Coal Industry. Journal of the Polish Mineral Engineering Society, No.2, Vol.1, 2021, http://doi.org/10.29227/IM-2021-02-56.
5. Zhou, Y. J., Xu, X. D., Li, X. T., Li, M., and Yang, Y. G.,2018. Study on catastrophe instability of support system in gypsum goaf based on energy dissipation theory. Adv. Civ. Eng. 2018, 1–9. doi:10.1155/2018/4293584.
6. Ma, C. Q., Li, H. Z., and Zhang, P. P., 2017. Subsidence prediction method of solid backfilling mining with different filling ratios under thick unconsolidated layers. Arab. J. Geosci. 10 (23), 511–512. doi:10.1007/s12517-017-3303-7
7. Sun, Q., Zhang, J. X., Zhou, N. 2018. Study and discussion of short-strip coal pillar recovery with cemented paste backfill. Int. J. Rock Mech. Min. Sci. 104, 147–155. doi:10.1016/j.ijrmms.2018.01.031
8. Chi, Y., C., Sheng, G. C., Chang, C. Zh., Shu, Y. D., Jiang, L., Yang, L., 2023. Research on cemented artificial pillars to replace protective inter-block coal pillars and stope failure laws. Original research article, Front. Earth Sci., 18 January 2023, Sec. Structural Geology and Tectonics, Volume 10 - 2022. https://doi.org/10.3389/feart.2022.1039478.
9. Niełacny P., 2009, Dobór technologii utrzymywania wyrobisk przyścianowych w jednostronnym otoczeniu zrobów na podstawie pomiarów przemieszczeń górotworu, Praca doktorska, Akademia Górniczo-Hutnicza, Krakowie, Poland.
10. Rak Z., 2017. Dobre praktyki w utrzymywaniu wyrobiska w jednostronnym otoczeniu zrobami zawałowymi. Zeszyty Naukowe, Instytut Gospodarki Surowcami Mineralnymi Polskiej Akademii Nauk, Poland, nr 101, pp. 117–132.
11. Reed, G., Mctyer, K., Frith, R., 2017, "An assessment of coal pillar system stability criteria based on a mechanistic evaluation of the interaction between coal pillars and the overburden", International Journal of Mining Science and Technology 27 (2017), pp. 9-15.
12. Simon, H. P., Muhammad, A. I., Ganda, M. S., Ridho, K. W., Irwandy, A., Made, A. R.,2019. New coal pillar strength formula considering the effect of interface friction. International journal of Rock Mechanics and Mining Sciencess 123 (2019) 104102.
13. Bieniewski, Z. T., 1992. A method revisited: Coal pilllar strength formula based on field investigations. Proceeding of the Workshop on coal pillar mechanics and design, Bu mines, pp. 158-165. (https://www.arcc.osmre.gov/resources/impoundments/BoM-IC-9315-Proceedingsof the Workshopon Coal Pillar Mechanicsand Design-Bieniawski1992.pdf).
14. Kang, Zh., Zhong, Q. G., Xiao,D. Z., Ze, M.Z., Xiao, J. W., 2013. Study on Stability of Metal Mine Overlying Strata for Artificial Pillar Support. IJCSI International Journal of Computer Science Issues, Vol. 10, Issue 1, No 2, January 2013. ISSN (Print): 1694-0784 | ISSN (Online): 1694-0814. www.IJCSI.org
15. Bui, M.T., Le, T.D., Liu. C.Y., Pham, V.C., 2020. Study on controlling parameters and technological optimization of Strip Longwall Top Coal Caving in thick coal seams. Inżynieria Mineralna – Journal of the Polish Mineral Engineering Society. 2020;46(2): 105-113.